ELSEVIER

14 February 1994

PHYSICS LETTERS A

Physics Letters A 185 (1994) 327–332

Intra-cavity laser resonance spectroscopy of hydrogen-like silicon ions

S.N. Lea [1], W.A. Hallett, A.J. Varney, C.T. Chantler [2], P.E.G. Baird, J.D. Silver

Department of Physics, Clarendon Laboratory, University of Oxford, Oxford, OX1 3PU, UK

A.R. Lee

Physics Department, La Trobe University, Bundoora, Victoria 3083, Australia

J. Billowes

Department of Physics, Manchester University, Manchester, M13 9PL, UK

Received 12 October 1992; revised manuscript received 14 December 1993; accepted for publication 15 December 1993
Communicated by B. Fricke

Abstract

The $2^2S_{1/2}$–$2^2P_{3/2}$ transition at 734 nm in the hydrogen-like ion Si^{13+} is studied by intra-cavity cw laser resonance spectroscopy of ions in a fast beam.

1. Introduction

Precision measurement of the 2S Lamb shift in hydrogen-like one-electron ions of medium-to-high atomic number Z is currently considered to be the best method of investigating quantum-electrodynamics (QED) in the approach to the strong field regime [1,2]. In the range $9 \leqslant Z \leqslant 18$, the $2^2S_{1/2}$–$2^2P_{3/2}$ transition in such ions (and also the $2^2S_{1/2}$–$2^2P_{1/2}$ transition at the higher-Z end of the range) lies in the wavelength range accessible to the techniques of laser spectroscopy. QED effects account for 4% of the $2^2S_{1/2}$–$2^2P_{3/2}$ transition energy, the bulk coming from the Lamb shift of the $2^2S_{1/2}$ state. The contribution of the $2^2P_{3/2}$ state is an order of magnitude smaller. The leading QED contribution to the Lamb shift, the order α self-energy, has been calculated to high numerical precision by Mohr [3,4]. The complete $n=2$ level energies and splittings, including all calculated contributions, have been tabulated [5,6]. It should be noted that Mohr's most recent results [4] are in agreement with his earlier calculations but have much reduced uncertainty estimates in the medium-Z, where the leading uncertainty is now that arising from fourth-order (α^2) QED terms.

The most recent and precise measurements of the $2^2S_{1/2}$–$2^2P_{3/2}$ transition energy, in S^{15+} [7] and P^{14+} [8], both show departures of about two experimental standard deviations from the theoretical values, supporting a trend for measurements of the 2S Lamb

[1] Present address: Laboratoire de Spectroscopie Hertzienne de l'Ecole Normale Supérieure, 24 rue Lhomond, 75231 Paris cedex 05, France.

[2] Present address: Quantum Metrology Division, National Institute of Standards and Technology, Gaithersburg, MD 20899, USA.

Elsevier Science B.V.
SSDI 0375-9601(93)E1008-4

shift to lie at values around 0.5% smaller than predicted [9]. The measurements [7,8] were both made by resonance spectroscopy of ions in a fast beam, using pulsed dye lasers. The leading systematic error is the uncertainty in the Doppler shift of the transition wavelength, owing to the high velocity ($\beta = v/c \sim 0.1$) of the ions. Systematic errors in wavelength and energy measurement, inherent in the use of pulsed lasers, can also be overcome by employing a cw laser.

These considerations have prompted the development of a cw intra-cavity laser resonance technique, which could ultimately enable errors from the ion beam velocity to be eliminated [10,11]. This Letter presents an observation, using this technique, of the $2^2S_{1/2}$–$2^2P_{3/2}$ transition in Si^{13} at 734 nm.

2. Outline of the experiment

The energy levels and radiative transitions of a hydrogen-like ion for $n = 1, 2$ are shown in Fig. 1. Stimulated resonance experiments in the $n = 2$ states are possible because the $2^2S_{1/2}$ level is metastable (16 ns lifetime in Si^{13+} [12]). Ions in the $2^2S_{1/2}$ level are resonantly excited by the laser radiation to the $2^2P_{3/2}$ level, from which they decay promptly by emission of a 2 keV Lyman-α X-ray. The laser resonance profile of the $2^2S_{1/2}$–$2^2P_{3/2}$ transition can be monitored by observing the X-ray rate as a function

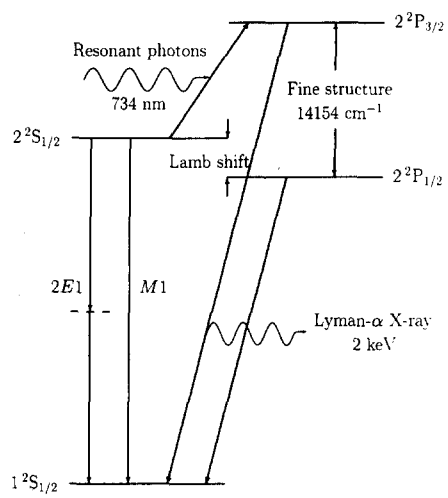

Fig. 1. Energy levels and radiative transitions of the $n = 1, 2$ states of the hydrogen-like ion Si^{13+} in the presence of the laser field.

of the laser frequency. The resonance is broad (129 cm^{-1} in Si^{13+}) because of the short lifetime of the 2^2P levels. Fig. 1 also indicates the two-photon (2E1) and magnetic dipole (M1) decays of the $2^2S_{1/2}$ level. For Si^{13+}, the M1 transition accounts for only 1% of the $2^2S_{1/2}$ level decay rate and the dominant 2E1 transition is the principal source of background X-ray radiation.

This experiment was performed at the tandem Van de Graaff accelerator of the SERC Nuclear Structure Facility (NSF) at Daresbury, UK. A sketch of the experimental set-up is given in Fig. 2. The relatively large silicon ion flux (up to 1 μA electrical of Si^{9+} at the accelerator exit) which was available at suitable energies (150–200 MeV) was one of the chief factors determining the choice of element. After excitation to the metastable hydrogen-like state, the ion beam was permitted to drift a distance of 42 cm, corresponding to slightly less than one $2^2S_{1/2}$ state lifetime, minimizing the X-ray background from short-lived states, to a focus determined by a quadrupole magnet several metres upstream. At this focus, 1 mm high by 5 mm broad, the ion beam passed through an interaction cell mounted in the long arm of a Coherent 599 three-mirror dye laser. The laser beam had a $1/e^2$ radius of 0.35 mm at the interaction region. For the data presented below, the ion beam intersected the dye laser beam at right angles (± 0.2 mrad). The dye employed was Pyridine-2, pumped by the multiline visible light of a Coherent CR-15 argon-ion laser. The intra-cavity laser power was monitored by a photo-diode picking up the reflected power from one of the Brewster-angle windows of the interaction cell. This photo-diode was calibrated against the transmitted power obtained using a cavity end mirror of known transmission, which was replaced by a high-reflectivity mirror during data-taking. The intra-cavity power was typically 48 W.

X-ray emission from the ion beam was observed by two gas-flow (90% Ar–10% CH_4) proportional

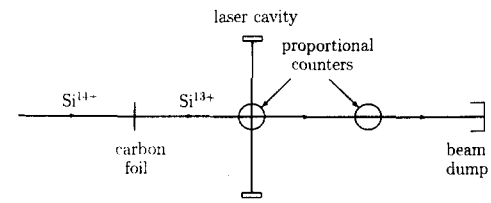

Fig. 2. Schematic plan of the experiment.

counters, one located above the ion-laser interaction region and the other 21 cm further downstream. The detection efficiency (solid angle and proportional counter efficiency) for 2 keV X-rays was $\eta \approx 7 \times 10^{-3}$ and for the 2E1 background, $\eta_B \approx 2 \times 10^{-3}$. The laser light was chopped at a nominal frequency of 500 Hz by a chopper wheel inside the cavity. After amplification and discrimination, the analogue signals from the proportional counters were digitized and routed into "laser on" and "laser off" pulse-height spectra, $S_{on}(E)$ and $S_{off}(E)$. The routing was determined by a CAMAC-based, PC-AT controlled, phase-sensitive detection system, which produced gating and routing pulses of equal length. The start of each on/off routing cycle was triggered by a photo-diode registering the laser coming "on", thus the start of each cycle was locked to the chopper-wheel frequency but the duration of each data-taking "window" was determined by the CAMAC timing, which was based on a quartz clock. When tested "off-line" with a calibration X-ray source (^{55}Fe) the whole system was free from signal differences due to timing errors at the level of 10^{-6}. The same routing and gating procedure was applied to the laser power and ion beam current monitors, providing normalization data.

3. Metastable state production

During the course of this experiment, silicon ion beams of 150, 170 and 200 MeV were used, with a variety of excitation conditions for the production of metastable Si^{13+} ions. The optimum $2^2S_{1/2}$ yield with the minimum of contamination from lower charge states was obtained with an accelerator terminal potential of 17 MV. The dominant charge state within the accelerator was Si^{9+}; the ions attaining a final energy of 170 MeV. The beam was stripped at the accelerator exit terminal by a carbon foil of nearly equilibrium thickness (70 μg/cm^2). Approximately 30% of the stripped ions originating from the Si^{9+} charge state were bare Si^{14+} nuclei; these ions were selected by the accelerator's analysing magnet and delivered to the experimental area. Before the interaction region, ions were prepared in the metastable $2^2S_{1/2}$ level of the Si^{13+} charge state by electron capture from a second, thin carbon foil (23 or 35 μg/cm^2).

A typical proportional counter spectrum obtained under these conditions is shown in Fig. 3. The energy calibration was performed using X-ray fluorescence from a number of medium-Z targets illuminated by Mn-K X-rays from a ^{55}Fe source. The identification of this spectrum as that of the 2E1 decays is supported by analysis of its shape. The rate for the 2E1 decay of the metastable state is $\gamma_s^{2E1} = 6.155 \times 10^7\ s^{-1}$ [12]. The total spectral background rate can be considered as the sum of the 2E1 decay rate, the M1 decay rate and a residual Lyman-α background at 2 keV.

In order to extract the probability with which the $2^2S_{1/2}$ level is populated, a modelled 2E1 spectrum, convolved with the Gaussian detector resolution and spectral efficiency function, is generated and subtracted from the data. Its amplitude is iterated until the subtraction results in zero counts in several channels in the region 1.0–1.5 keV (solid line in Fig. 3). When this condition is satisfied, the area of the model spectrum (dashed line in Fig. 3) provides an estimate of the detected number of 2E1 X-rays whilst the altered data contains the residual spectrum. This residual spectrum is similar to that expected for a 2 keV Lyman-α X-ray. It contains a substantial component of (laser-unrelated) Lyman-α background due to electron capture from residual gas in the beamline. From the intensity of the 2E1 spectrum, the probability of populating $2^2S_{1/2}$ by this method is estimated at 0.6(3)%. This is about half the prediction of a simple model of the capture process [13] and a factor of five smaller than the probability inferred from other data taken under similar conditions [14].

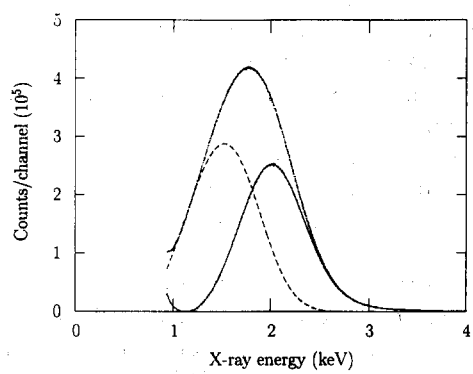

Fig. 3. Typical proportional counter spectrum (dotted line). Also shown is the residual 2keV X-ray background peak (solid line) obtained by subtraction of a scaled modelled 2E1 spectrum (dashed line) from the original data.

The probability of population of metastable states in helium-like Si^{12+} by double electron capture from the foil is demonstrated to be negligible by comparison with X-ray spectra obtained when a Si^{8+} or Si^{10+} beam is incident on the foil, in which the 1.85 keV X-ray decay of the metastable 2^3P_2 level in Si^{12+} is clearly visible [15].

The ratio of the 2E1 count rate to the residual count rate, corrected for the relative efficiency of the proportional counters over the two components of the spectra is around 3–5. The deduced 2E1 fraction could, however, be considerably larger for only a small change in the detector calibration. However, the metastable ion flux and the residual Lyman-α rate deduced from the proportional counter spectra are, within their errors, in crude agreement with the expected rates for these beam conditions.

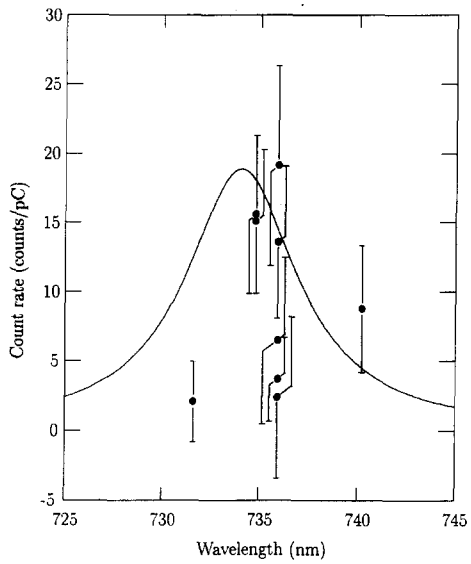

Fig. 4. Fit of the resonance data to the theoretical lineshape. The curve is a Lorentzian with 6.9 nm linewidth, centred at the expected resonance wavelength of 734 nm.

4. Laser resonance data

Nine three-hour experimental runs were made at four laser wavelengths within the FWHM (7 nm) of the expected resonance at 734 nm in the ion rest frame. Each run consists of 5×10^6 cycles; the laser "on" time in each cycle is 900 μs, giving a total laser "on" time of 9×10^3 s. The $1/e^2$ radius of the laser beam in the plane of interaction is 350(50) μm, which for the ion beam velocity of $\beta=0.114$ gives an interaction time $\tau=1.0(2)\times10^{-11}$ s. The laser intensity is $I=1.3(3)\times10^8$ Wm. The difference spectrum, $S_{dif}(E)=S_{on}(E)-S_{off}(E)$, is formed for each run. These difference spectra are consistent with a peak at the Lyman-α energy; however, repeated runs at the same wavelength show some scatter in the strength of the resonance. The difference spectra are integrated over the range 1.5–2.5 keV and are normalized to the integrated beam current for each run. The resulting count rates for the nine experimental runs are plotted in Fig. 4.

The observed resonance strength can be compared with that predicted by an analysis of the resonance process. For cw laser radiation, a time-dependent perturbation theory method [16] can be used to show that the $2^2S_{1/2}$–$2^2P_{3/2}$ transition rate *per ion* induced by a laser field of intensity I leads to a Lyman-α rate on resonance of

$$A_{\text{Ly-}\alpha}=\frac{48\pi\alpha}{\hbar\gamma_p}\left(\frac{a_0}{Z}\right)^2 I=4.66\times10^4 Z^{-6} I\,\text{s}^{-1}, \qquad (1)$$

where $\gamma_p=6.27\times10^8 Z^4\,\text{s}^{-1}$ is the Lyman-α decay rate, a_0 is the radius of the first Bohr orbit in hydrogen and α is the fine structure constant (SI units are assumed in calculating the numerical factor). Eq. (1) demonstrates that resonance experiments are intrinsically more difficult, i.e. require higher laser power, at higher Z, independently of the difficulty of obtaining laser radiation at shorter wavelengths.

The observed signal rate can be compared to that predicted by Eq. (1). Combining the results of the five runs showing the strongest resonances yields a total of $106(19)\times10^3$ resonant counts. The integrated beam current was 9(4) mC of ion beam, corresponding to $N(2s)\approx2.3(1.0)\times10^{13}$ metastable ions at the interaction region. An experimental value for the single-ion transition probability can be obtained,

$$P_{\text{exp}}=\frac{\int S_{\text{dif}}(E)\,dE}{N(2s)\eta_S}\approx6(3)\times10^{-7}, \qquad (2)$$

which can be compared with the theoretical probability $P_{\text{th}}=A_{\text{Ly-}\alpha}\tau\approx8(2)\times10^{-6}$.

The discrepancy, together with the variation of the

resonance data, can be understood by consideration of the laser and ion beam interaction geometry. The Lyman-α decay rate is $R_S = A_{Ly\text{-}\alpha}\Phi\tau G\eta_S$, where Φ is the flux of metastable ions, τ their time-of-flight through the laser beam, η_S is defined above and G is a geometrical volume factor for the overlap of the laser and ion beams, analysis of which shows that the signal rate can be halved by movements of 140 μm of the ion beam relative to the laser beam. Maintaining the transverse position of an ion beam focus to better than this fraction of its diameter is a demanding requirement in the absence of more sophisticated beam position sensing diagnostics than were available for this experiment and it can be inferred that transverse position drifts of this order of magnitude are responsible for the variation of the resonance data. In addition, a larger ion beam size can easily account for the smaller than predicted transition probability.

Fig. 4 illustrates the resonance data in the light of this analysis. The five runs at 735.9 nm show resonances ranging from 2 to 19 counts/pC, with a statistical uncertainty of about ±6 counts/pC for each measurement. For the ion and laser beam widths quoted above, the change between the strongest and weakest resonance at this wavelength can be accounted for by an ion beam movement of 1.5 $1/e^2$ laser beam radii (0.5 mm) between the runs. The largest resonance rate can be taken as being the closest approach to the condition of the laser and ion beams intersecting on axis. Fig. 4 includes a Lorentzian of 6.9 nm FWHM centred at 734 nm (the expected theoretical line profile) for comparison with the data.

5. Developments

The present experiment was performed with the laser and ion beams intersecting perpendicularly. Under these circumstances the resonance wavelength is shifted in the laboratory frame by the second-order Doppler shift only; the uncertainty in the resonance wavelength, $\Delta\lambda$, due to the Doppler shift can be expressed as $\Delta\lambda = \lambda_0\gamma(\beta\Delta\theta + \Delta\beta)$, where λ_0 is the resonance wavelength in the ion's rest frame, $\beta = v/c$ where v is the ion velocity, $\gamma = (1-\beta^2)^{-1/2}$, and $\Delta\beta$ and $\Delta\theta$ are the uncertainties in the ion velocity and the intersection angle respectively.

If the problems associated with ion beam movement can be overcome, and if higher intra-cavity laser power can be obtained (using e.g. a Ti:sapphire laser or a diode laser coupled to a feedback enhancement cavity) then the intra-cavity cw laser resonance technique offers the possibility of eliminating both the first- and second-order Doppler shift from the extraction of the resonance wavelength. The cavity can be considered as a containing two counter-propagating laser beams. If the cavity is set at an angle θ to the ion beam (not far from 90°) and the laser is tuned over a large enough bandwidth, two resonances can be observed, centred at Doppler-shifted wavelengths $\lambda_\pm = \lambda_0\gamma(1 \pm \beta\cos\theta)$. By summing and differencing these shifted wavelengths, the ion beam velocity can be eliminated from the evaluation of the rest frame wavelength to first and second order,

$$\lambda_0 = \tfrac{1}{2}[(\lambda_+ + \lambda_-)^2 - (\lambda_+ - \lambda_-)^2\cos^2\theta]^{1/2}. \qquad (3)$$

Thus all dependence of the final result on the ion beam energy is eliminated, avoiding systematic errors arising from energy loss in the stripping and exciting foils or differences in velocity between ions of different charge states. It may be noted that in the case where the laser beam is aligned along the ion beam axis ($\theta = 0$), the rest frame wavelength is given simply by $\lambda_0^2 = \lambda_+\lambda_-$.

A similar method for eliminating the Doppler shift from measurements made using pulsed lasers has recently been described [17].

6. Conclusions

Laser-induced $2^2S_{1/2}$–$2^2P_{3/2}$ transitions in Si^{13+} have been observed at wavelengths consistent with current calculations of the transition energy, by detection of the prompt X-ray decay from the $2^2P_{3/2}$ state. A development of the method to enable the uncertainty in the ion beam velocity to be eliminated from a final measurement of the transition energy has been described.

Acknowledgement

We wish to thank the former staff of the Daresbury NSF accelerator and in particular Dr W. Gelletly for

kindly making available to us a period of director's discretionary beam time in the early stages of this experiment. We are grateful to B. Couillaud and K. Ibbs of Coherent Inc. in Palo Alto for advising us on our choice of laser system and for lending us a set of mirrors for the dye laser. We acknowledge fruitful discussions with Professor D.D. Dietrich and H.S. Margolis during the course of this work. Three of us (SNL, WAH, AJV) acknowledge the SERC for the award of postgraduate research studentships for this work whilst CTC thanks St Anne's College, Oxford, for a Junior Research Fellowship.

References

[1] P.J. Mohr, in: Physics of strong fields, ed. W. Greiner (Plenum, New York, 1987) p. 17.
[2] A. van Wijngaarden, J. Patel and G.W.F. Drake, in: Atomic physics 11, eds. S. Haroche, J.C. Gay and G. Grynberg (World Scientific, Singapore, 1989) p. 355.
[3] P.J. Mohr, Ann. Phys. (NY) 88 (1974) 26, 52; Phys. Rev. Lett. 34 (1975) 1050; Phys. Rev. A 26 (1982) 2338.
[4] P.J. Mohr, Phys. Rev. A 46 (1992) 4421.
[5] P.J. Mohr, At. Data Nucl. Data Tables 29 (1983) 453.
[6] W.R. Johnson and G. Soff, At. Data Nucl. Data Tables 33 (1985) 405.
[7] A.P. Georgiadis, D. Müller, H.-D. Sträter, J. Gassen, P. von Brentano, J.C. Sens and A. Pape, Phys. Lett. A 115 (1986) 108.
[8] J. Gassen, D. Müller, D. Budelsky, L. Kremer, H.-J. Pross, P. von Brentano, A. Pape and J.C. Sens, Phys. Lett. A 147 (1990) 385.
[9] P. Pellegrin, Y. El Masri and L. Palffy, Phys. Rev. A 31 (1985) 5;
V. Zacek, H. Bohn, H. Brum, T. Faestermann, F. von Feilitzsch, G. Giorginis, P. Kienle and S. Schuhbeck, Z. Phys. A 318 (1984) 7;
O.R. Wood, C.K.N. Patel, D.E. Murnick, E.T. Nelson, M. Leventhal, H.W. Kugel and Y. Niv, Phys. Rev. Lett. 48 (1982) 398;
H. Gould and R. Marrus, Phys. Rev. A 28 (1983) 2001.
[10] R.A. Holt, S.D. Rosner, T.D. Gaily and A.G. Adam, Phys. Rev. A 22 (1980) 1563.
[11] J.D. Silver, in: The hydrogen atom, eds. G.F. Bassani, M. Inguscio and T.W. Hänsch (Springer, Berlin, 1989) p. 221.
[12] F.A. Parpia and W.R. Johnson, Phys. Rev. A 26 (1982) 1142.
[13] H.W. Kugel and D.E. Murnick, Rep. Prog. Phys. 40 (1977) 299.
[14] H.-D. Betz, D. Röschenthaler and J. Rothermel, Phys. Rev. Lett. 50 (1983) 34.
[15] S.N. Lea, D.Phil. thesis, University of Oxford (unpublished, 1991).
[16] P. Kusch and V.W. Hughes, in: Handbuch der Physik, ed. S. Flügge (Springer, Berlin, 1959) 37/1 §§31, 71–73.
[17] D. Müller, J. Gassen, F. Scheuer, H.-D. Sträter and P. von Brentano, Z. Phys. D 18 (1991) 249;
P. von Brentano, D. Platte, D. Budelsky, L. Kremer, H.-J. Pross and F. Scheuer, Phys. Scr. T 46 (1993) 162.